(1)

Eighth Interim Report

STUDY OF METHODS OF IMPLEMENTING POYNTING VECTOR MEASUREMENTS

For the period

April 1 to June 30, 1964

UNIVERSITY of PENNSYLVANIA

The Moore School of Electrical Engineering

PHILADELPHIA, PENNSYLVANIA 19104

Eighth Interim Report

STUDY OF METHODS OF IMPLEMENTING POYNTING VECTOR MEASUREMENTS

For the period

April 1 to June 30, 1964

by

Nabil Farhat
K. S. Foo
R. M. Showers

Contract NBy-32219

between

U. S. Naval Civil Engineering Laboratory
Port Hueneme, California

and

The Moore School of Electrical Engineering
University of Pennsylvania
Philadelphia, Pa. 19104

July 31, 1964

Moore School Report No. 65-07

TABLE OF CONTENTS

LIST OF ILLUSTRATIONS

STUDY OF METHODS OF IMPLEMENTING POYNTING VECTOR MEASUREMENTS

1.0 INTRODUCTION

The contents of this report consist of the results of a number of experiments with the "Poynting Sensor" at a frequency of 1 Mc. The purpose of these experiments, described in the last interim report,[1] was to verify the feasibility of making Poynting vector measurements in the near field at 1 Mc. The measurements included magnitude measurement of the E and H components of the field and their relative time phase. Phase measurement was performed with the aid of an oscilloscope and also through the use of a transistorized phase-meter which was expected to provide easier and better measurement accuracy. Multiplication of the magnitudes of E and H by cos γ (where γ is the relative angle between them) is also described. This was achieved through the use of a square law multiplier which provided a simple but effective means of measuring the Poynting vector directly. The report presents a description of the new instrumentation used, measurement techniques and a brief discussion of the ground plane and its bearing on the measurement at 1 Mc. Photographs of the instrument assemblies used in performing these measurements are also given (Figs. 16-19).

2.0 MEASUREMENT OF POYNTING VECTOR UTILIZING SQUARE LAW MULTIPLICATION

a) Theoretical Considerations

Consider two sinusoidal signals e_{S1} and e_{S2} of the same frequency ω with a relative phase difference γ between them, connected in series to the input terminals of a nonlinear element as shown in Fig. 1.

If one writes:

$$e_{S1} = A \cos \omega t \tag{1}$$

$$e_{S2} = B \cos (\omega t + \gamma) \tag{2}$$

and assumes that the characteristic of the nonlinear element can be sufficiently approximated by the first three terms in the power series expansion, i.e.

$$e_o = a_o + a_1 e_{in} + a_2 e_{in}^2 + \cdots \tag{3}$$

then one readily finds by substitution of

$$e_{in} = e_{S1} + e_{S2} \tag{4}$$

into eq. (3)

$$e_o \simeq a_o + a_1 A \cos \omega t + a_1 B \cos(\omega t + \gamma) + a_2 \left\{ A^2 \cos^2 \omega t + \right.$$
$$\left. + \underline{2 AB \cos \omega t \cos(\omega t + \gamma)} + B^2 \cos^2(\omega t + \gamma) \right\} + \tag{5}$$

The underlined term in eq. (5) can be expanded into

$$2a_2 AB \cos \omega t \cos(\omega t + \gamma) = a_2 AB \cos 2\omega t + a_2 AB \cos \gamma \tag{6}$$

in which $a_2 AB \cos \gamma$ is a dc term. The total dc voltage appearing at the output terminals of the nonlinear element can now be easily isolated through the use of a low-pass filter with a cutoff frequency below the radian frequency ω, with the result that one obtains a dc voltage at the output given by

$$e_{o_{dc}} \simeq a_o + a_2 AB \cos \gamma \tag{7}$$

It is evident that this voltage is proportional to the product of the magnitude of the two input signals by the cosine of the time phase difference

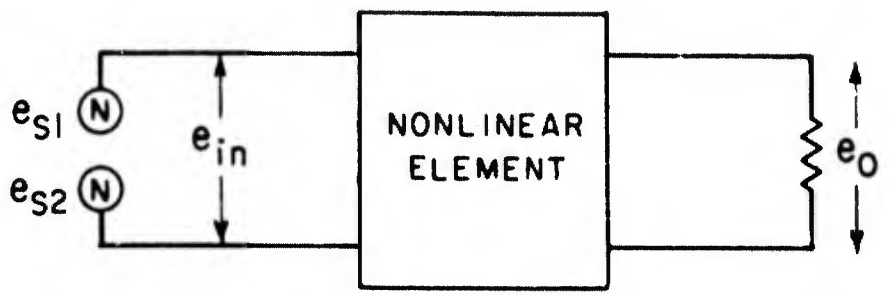

FIG. 1. NONLINEAR ELEMENT MULTIPLICATION

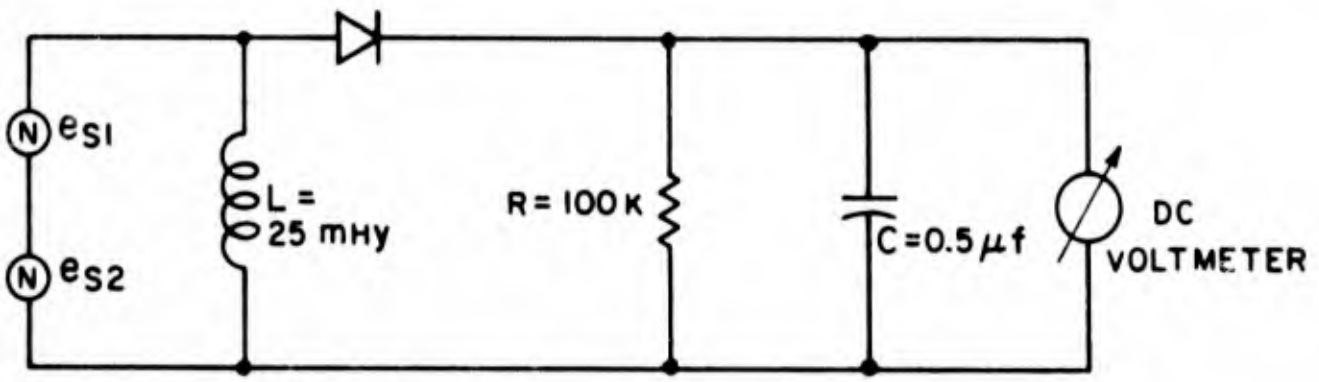

FIG. 2. CIRCUIT DIAGRAM OF SQUARE LAW MULTIPLIER

between them. When A and B are synonymous or proportional to the components of the field E and H, the dc voltage in eq. (6) will be proportional to the magnitude of the Poynting vector.

b) Implementation

A practical circuit for the nonlinear element (square law) multiplier that was designed and built for use in conjunction with the two PRM-1 receivers is shown in Fig. 2. The voltages e_{S1} and e_{S2} are obtained from the oscilloscope output terminals on the PRM-1 receivers. Their frequency is at an intermediate level of 455 kc and their magnitudes are proportional to the E and H components of the field detected by the loop and rod antennas feeding the receivers. Also, the relative phase between e_{S1} and e_{S2} is linearly proportional to the time phase between E and H. All the ac components appearing at the output terminals are short-circuited by the capacitor C. The purpose of the inductance L is to provide a dc return. In order to make use of the multiplier, it is necessary to determine the values of a_o and a_2 in eq. (7). This is easily accomplished by feeding two signals e_{S1} and e_{S2} with a relative time phase of $\gamma = 90^o$ into the multiplier. In accordance with eq. (7) the dc voltage measured then should give the value of a_o directly. Knowing the value of a_o, one can determine a_2 from eq. (7) by feeding e_{S1} and e_{S2} with known amplitudes and in phase coherence (i.e. $\gamma = 0$).

c) Calibration and Operational Test of the Multiplier

Since the time phase between the IF outputs of the two PRM-1 receivers can be adjusted by tuning the slave receiver,[1] the following method of calibration and test of the square law multiplier was adop Referring to Fig. 3, the unit oscillator is set at a frequency of 1

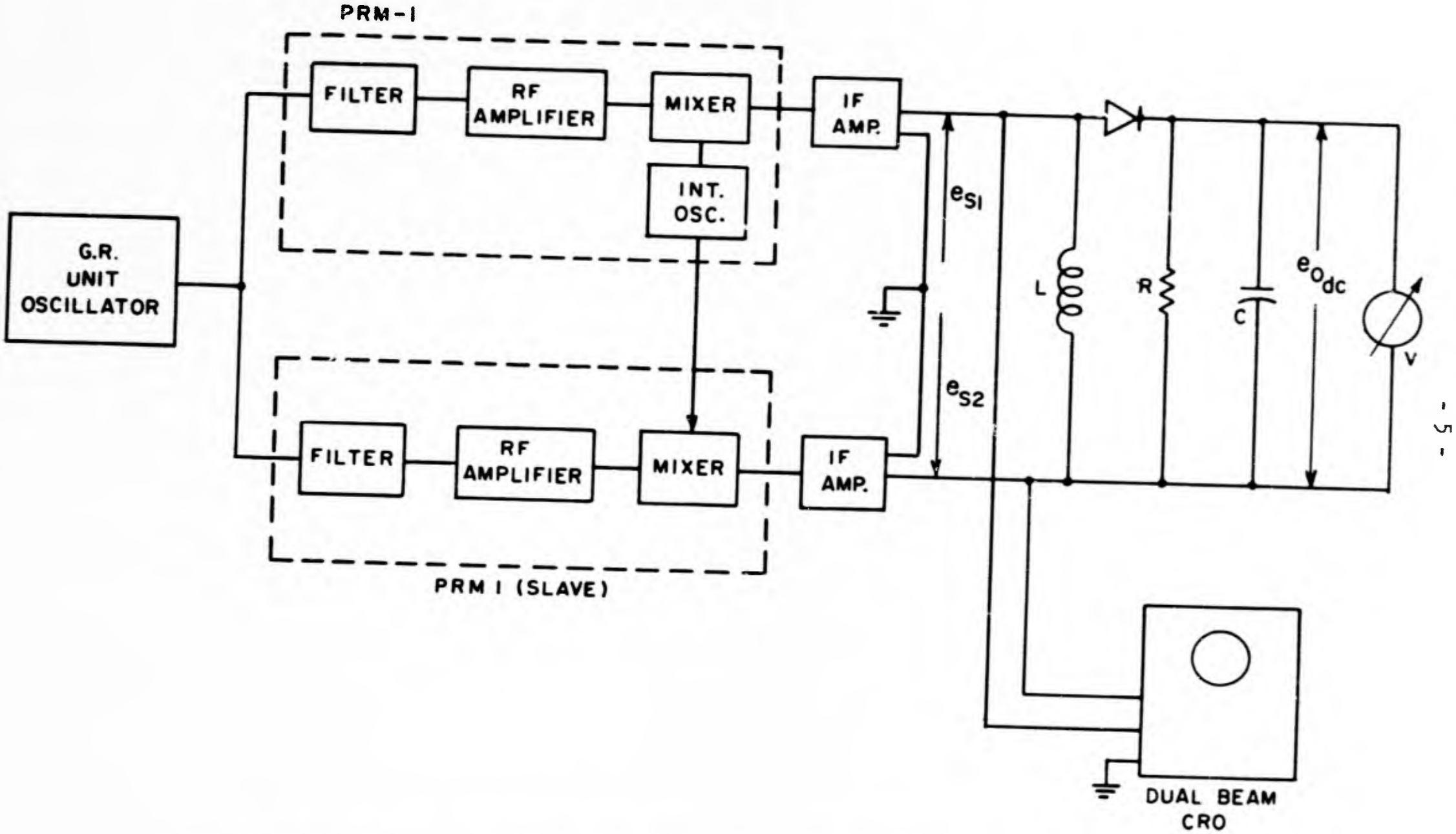

FIG. 3. SETUP FOR CALIBRATION AND TEST OF SQUARE LAW MULTIPLIER

and the receivers tuned to that frequency. The slave receiver is retuned next so that the IF output voltages e_{S1} and e_{S2} are in time phase γ with respect to each other. γ was monitored on the dual beam oscilloscope and was varied between 0° and 90° in steps of 10° each, and the dc output voltage $e_{o_{dc}}$ recorded. Since the magnitude of the IF voltage e_{S2} changes with retuning, the gain knob on the slave receiver was utilized to keep $e_{S2} = e_{S1}$ at all times. Results of measurements conducted with the multiplier for two different magnitudes of input signals are given in Tables I and II below. Table I is for $e_{S1} = e_{S2} = 0.96$ volt, and Table II is for $e_{S1} = e_{S2} = 2$ volts.

TABLE I

γ°	$e_{o_{dc}}$ (volts)	$e_{o_{dc}} - a_o$(volts)	0.19 cos γ	Remarks
0	0.38	0.19	0.19	$e_{S1} = e_{S2} - 0.96V$
10	0.375	0.185	0.187	
20	0.365	0.175	0.179	$a_o = 0.19$
30	0.35	0.16	0.165	$a_2 = 1.0$
40	0.33	0.14	0.145	
50	0.31	0.12	0.122	
60	0.30	0.11	0.095	
70	0.27	0.08	0.065	
80	0.225	0.035	0.033	
90	0.19	0.0	0.0	

TABLE II

γ^{o}	$e_{o_{dc}}$ (volts)	$e_{o_{dc}} - a_o$ (volts)	0.39 cos γ	Remarks
0	1.065	0.39	0.39	$e_{S1} = e_{S2} = 2V$
10	1.06	0.385	0.384	
20	1.04	0.365	0.367	$a_o = 0.675$
30	1.01	0.335	0.337	$a_2 = 0.0975$
40	0.98	0.305	0.299	
50	0.935	0.260	0.25	
60	0.88	0.205	0.195	
70	0.82	0.145	0.133	
80	0.75	0.075	0.068	
90	0.675	0.0	0.0	

The degree of accuracy of the multiplier is evident from comparison of the last two columns in both Tables I and II. The small discrepancies in the results are thought to be due to inaccuracies in the phase reading on the oscilloscope and to the approximation made in the assumed characteristic of the nonlinear element. From the results in Tables I and II, we note that the value of a_o and a_2 is dependent on the magnitude of the input signal due apparently to the shift in the dc operating point.

Figure 4 shows a_o and a_2 as a function of $(e_{S1} \times e_{S2})$ when $e_{S1} = e_{S2} = e_{S_{eq}}$. The curve applies with a small sacrifice in accuracy for the case of approximately equal inputs. For instance, deviation in e_{S1} and e_{S2}

FIG. 4. DEPENDENCE OF a_0 (IN VOLTS) AND a_2 (IN VOLTS^{-1}) ON INPUT SIGNALS TO MULTIPLIER

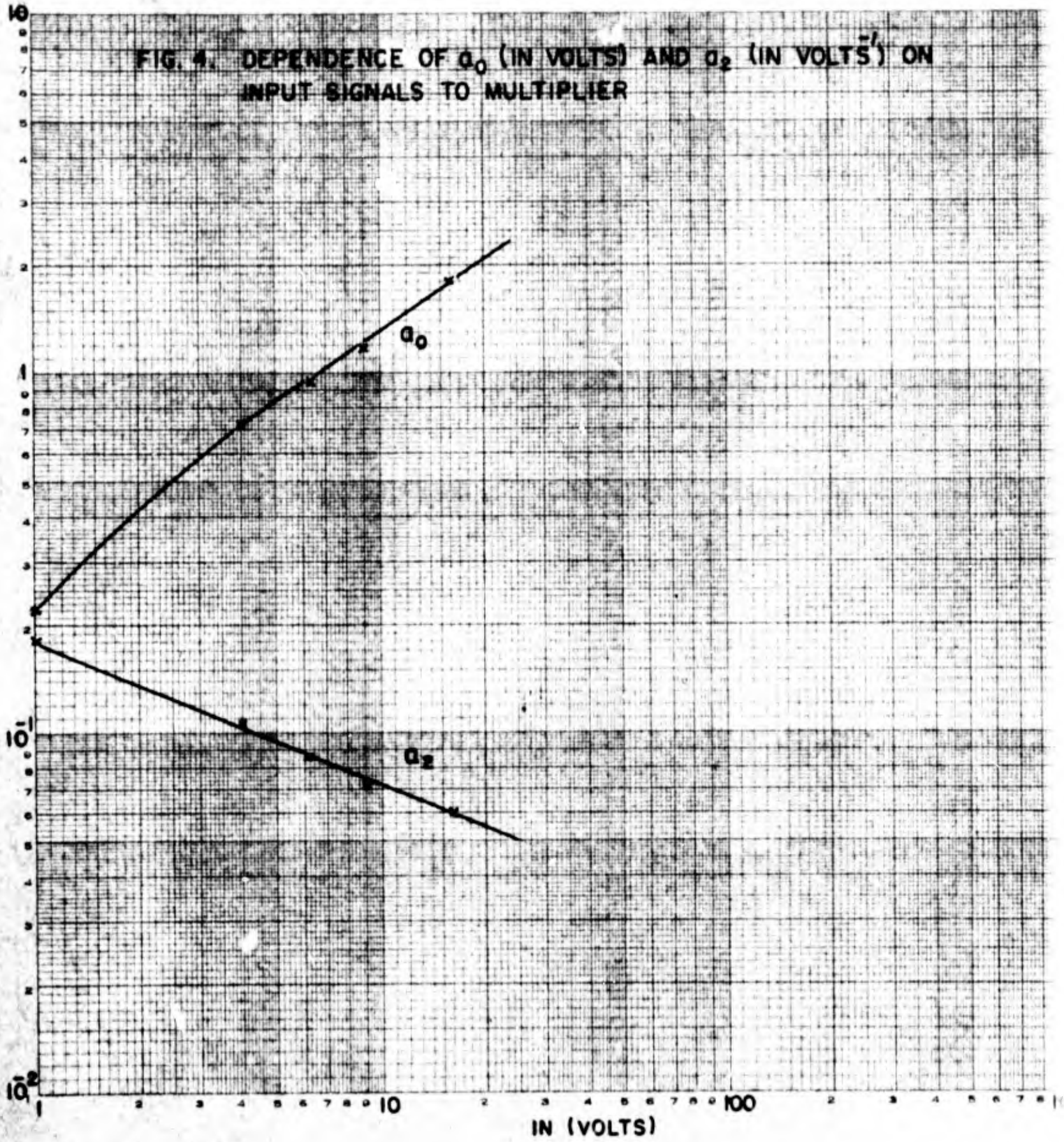

as large as 20% from $e_{S_{eq}}$ causes errors less than $\pm$ 5% and $\pm$ 8% in a_o and a_2 respectively from their values for the equal input case. The dependence of a_o and a_2 on the magnitudes of the input signals to the multiplier implies that the logical way of performing measurement with the multiplier is to keep e_{in_1} and e_{in_2} equal and constant at all times. It was therefore initially intended to maintain $e_{S_1} = e_{S_2}$ = constant, while the distance r between the transmitter and the receivers was changed (see Fig. 5). This could be achieved by calibrating the gain control on the PRM-1 receivers as continuously variable attenuators, which in conjunction with the step attenuators of the receivers (not shown in Fig. 5) can serve to keep e_{S1} and e_{S2} equal and constant over a wide distance range. A visual check on the phase between e_{S1} and e_{S2} and their magnitudes is provided by the oscilloscope in Fig. 5. Under this measurement scheme a quantity $|S|$ proportional to the magnitude of the Poynting vector can be obtained from the indication of the multiplier $e_{o_{dc}}$ through the formula:

$$|S| = \frac{e_{o_{dc}} - a_o}{a_2} \times \text{attenuation readings on receivers} \qquad (8)$$

Unfortunately, it was discovered that this method of measurement is not possible with the receivers at hand. It appears that while calibration of the gain knobs was perfectly feasible, changing the position of the step attenuator produced a small change in the phase between e_{S1} and e_{S2}. Rather than try to eliminate this effect which probably would require changes in the design of the receivers, it was decided to perform the measurement with a fixed position of the step attenuator and gain knobs, permitting e_{S1} and e_{S2} to change with distance. The actual measurement (and all the subsequent

field measurements described in this report) was performed in an open field in order to minimize the effect of reflections. The experimental setup used is that shown in Fig. 5. The dual beam scope was powered from a portable ac power pack, while the transmitter was powered from a mechanical inverter operating from a 12 V car battery. With the transmitter on and at a distance r = 30 m, the receivers were adjusted to provide $e_{S1} = e_{S2} = 1$ volt with an arbitrary phase difference between them. The reading of the multiplier $e_{o_{dc}}$ was next recorded as r was reduced in steps of 5 m each. Typical results of such a measurement are given in Table III which show that e_{S1} and e_{S2} remain nearly equal for each distance considered. Using Fig. 4 the values of a_o and a_2 are determined for the values of $(e_{S1} \times e_{S2})$ at each distance (column 6 and 7, Table III). The quantity $KV_E V_H \cos \gamma = e_{S1} e_{S2} \cos \gamma$ where V_E and V_H are the outputs of the rod and loop antennas respectively and K a proportionality constant is next computed from eq. 7, where $A = e_{S1} = K_1 V_E$ and $B = e_{S2} = K_2 V_H$. The results are given in column 8 of Table III. A plot of $(KV_E V_H \cos \gamma)$ vs distance (Fig. 6) shows a slope of approximately - 1.62 which is in the order of magnitude of the expected theoretical inverse square law dependence.

3.0 PHASE MEASUREMENT WITH THE OSCILLOSCOPE

A discussion of this measurement was given in the previous interim report.[1] However, the measurement as such was not performed then due to various difficulties in the actual measurement. Some of these difficulties were overcome through careful shielding and grounding. Also the use of a separate ac power plant for the oscilloscope proved to be very helpful.

The measurement was finally performed with a fair degree of success (i.e. within the accuracy of measuring phase difference with an oscilloscope)

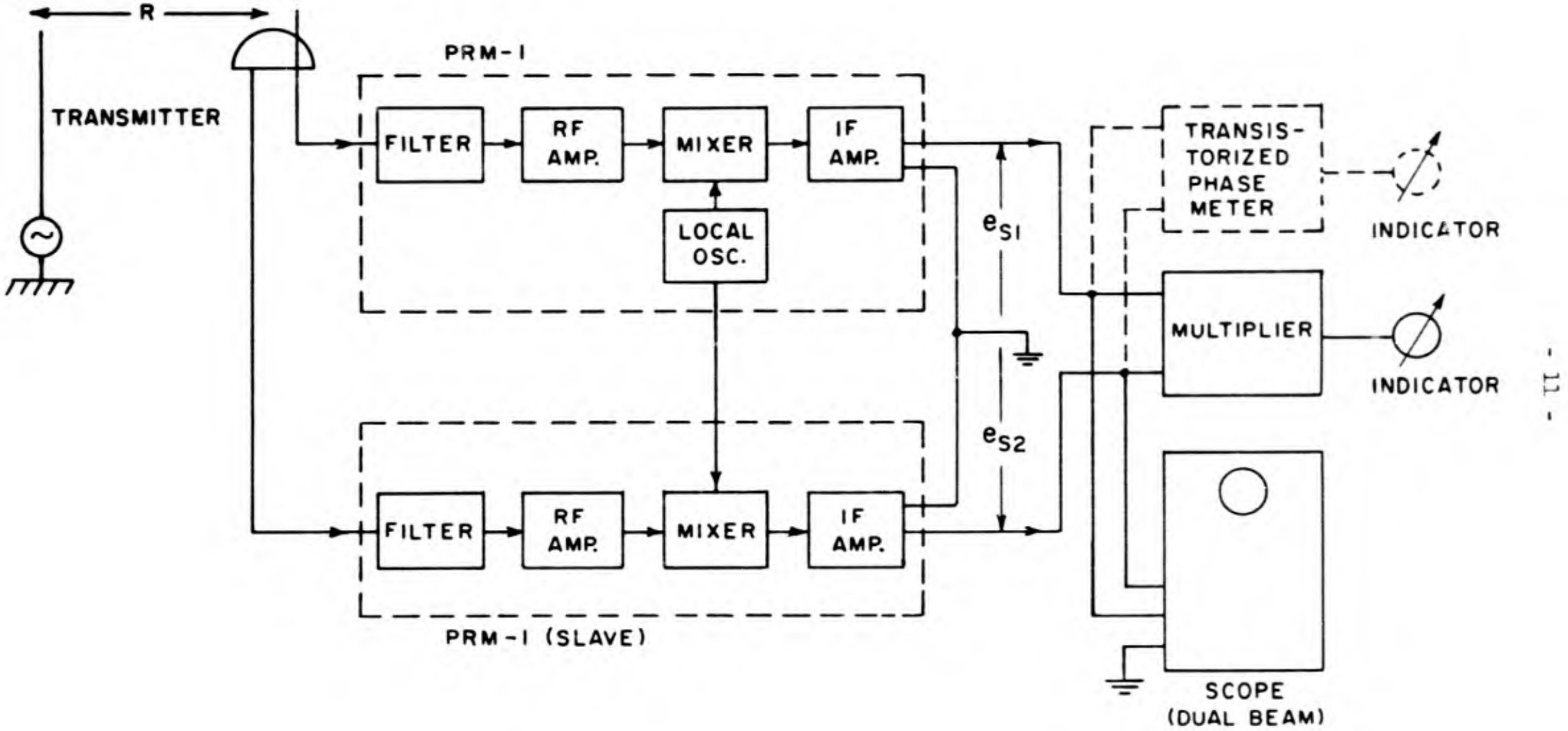

FIG. 5. EXPERIMENT SETUP FOR DIRECT MEASUREMENT OF THE MAGNITUDE OF THE POYNTING VECTOR

TABLE III

Data and Computation Table of the Quantity $KV_E V_H \cos \gamma$ Equal to the Magnitude of the Poynting Vector as Obtained from Multiplier

Distance r (meters)	$e_{S1} \alpha V_E$ (volts)	$e_{S2} \alpha V_H$ (volts)	Multiplier Output $e_{o_{dc}}$ (volts)	$(e_{S1} \times e_{S2})$ (volts)	a_o (volts)	a_2 (volts^{-1})	$KV_E V_H \cos \gamma = e_{S1} e_{S2} \cos \gamma = (e_{o_{dc}} - a_o)/a_2$
5	3.8	3	0.5	11.4	0.22	0.18	1.56
10	2.1	2.28	0.63	4.8	0.325	0.152	2.0
15	1.74	1.81	0.82	3.15	0.44	0.132	2.8
20	1.48	1.46	1.05	2.16	0.58	0.113	4.2
25	1.23	1.23	1.35	1.5	0.8	0.096	5.73
30	1.0	1.0	2.25	1.0	1.42	0.068	12.2

FIG. 6. VARIATION OF THE QUANTITY $KV_E V_H \cos\gamma = |p|$ WITH DISTANCE AS OBTAINED FROM MULTIPLIER

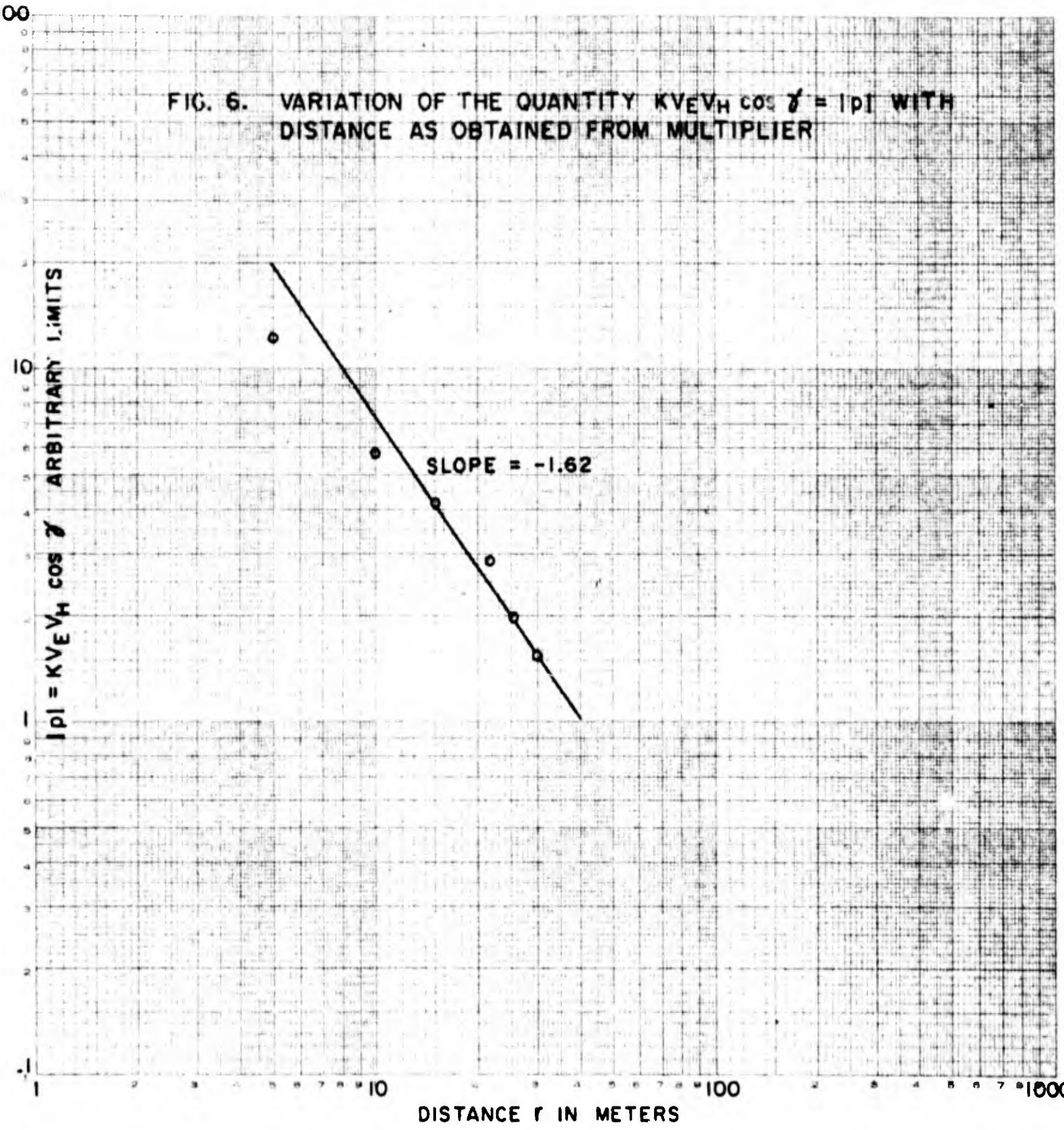

after the following modifications were introduced:

1. In order to minimize the effect of reflections from objects on the building roof where the measurement was first attempted, it was necessary to move all the instruments to an open site. Use was made of an available football field.

2. A dc/ac mechanical inverter operating from a rechargeable 12 V car battery was used to supply the transmitter. This eliminated the need for the very long stretches of ac power cables that were used before to supply the trarsmitter, and that proved to interfere with the measurement. The experimental setup used to perform the actual measurement, with the exception of the multiplier, is essentially that given in Fig. 5.

On attempting the measurement following the technique described in the previous report,[1] it was immediately discovered that the injection network that coupled the loop to one of the PRM-1 receivers introduced a certain amount of phase shift. Furthermore, the phase shift introduced by this network for injected signals through the injection terminal and the rod connection terminal were not identical. This fact ruled out the possibility of directly using this technique for accurate calibration without an extensive laboratory procedure for determining the appropriate correction factor. It was consequently decided to use an approximate calibration method instead. This method consisted of retuning the slave receiver when the [illegible]ensor was placed very close to the transmitting antenna to obtain [illegible]e of the IF outputs of both receivers by observing the traces o[illegible]-scope. The transmitter was next moved in steps of a few meters at [illegible]ime away from the sensor and the intensity of the loop and rod signals as measured

by the PRM-1 receivers was recorded. Also the phase as measured by the oscilloscope was recorded. Although this calibration method has the disadvantage of having the possibility of interaction error produced at the very close spacing of transmitter and receivers, it seemed to be the only meaningful way of measuring time phase variation with distance with this technique. The results of this measurement are given in Figs. 7, 8 and 9, which show fair agreement with the theory. The time phase angle φ measured by this method is given in Fig. 7. The actual time phase angle between E and H is $\gamma = 90 = \varphi$. This can be readily verified by inspection of equations (1.3.1), (1.3.2) and (1.3.3) given in the Fourth Interim Report[2] and repeated below:

$$E_r = \frac{|M|\beta^3}{4\pi\epsilon} \epsilon^{j\omega t} \left[\frac{2}{(\beta r)^2} + \frac{2}{j(\beta r)^3}\right] \cos\theta \qquad (9\text{-a})$$

$$E_\theta \frac{|M|\beta^3}{4\pi\epsilon} \epsilon^{j\omega t} \left[\frac{1}{j\beta r} + \frac{1}{(\beta r)^2} + \frac{1}{j(\beta r)^3}\right] \sin\theta \qquad (9\text{-b})$$

$$H_\varphi = \frac{\omega |M| \beta^2}{4\pi} \epsilon^{j\omega t} \left[-\frac{1}{j\beta r} + \frac{1}{(\beta r)^2}\right] \sin\varphi \qquad (9\text{-c})$$

The rod is oriented to measure only E_φ. From the two equations of E_θ and H_φ above, it is evident that E_θ and H_φ are about 90° out of phase in the very near field where only the higher order terms are considered. Furthermore, there is another 90° difference introduced by the loop, i.e. the voltage induced in the loop is 90° out of phase with the magnetic field H_φ. There is then a total of 180° time phase difference between the two voltages as the outputs of the PRM-1. However, a 180° time phase change can be effected by rotating the loop by 180° space phase; with this 180° change at

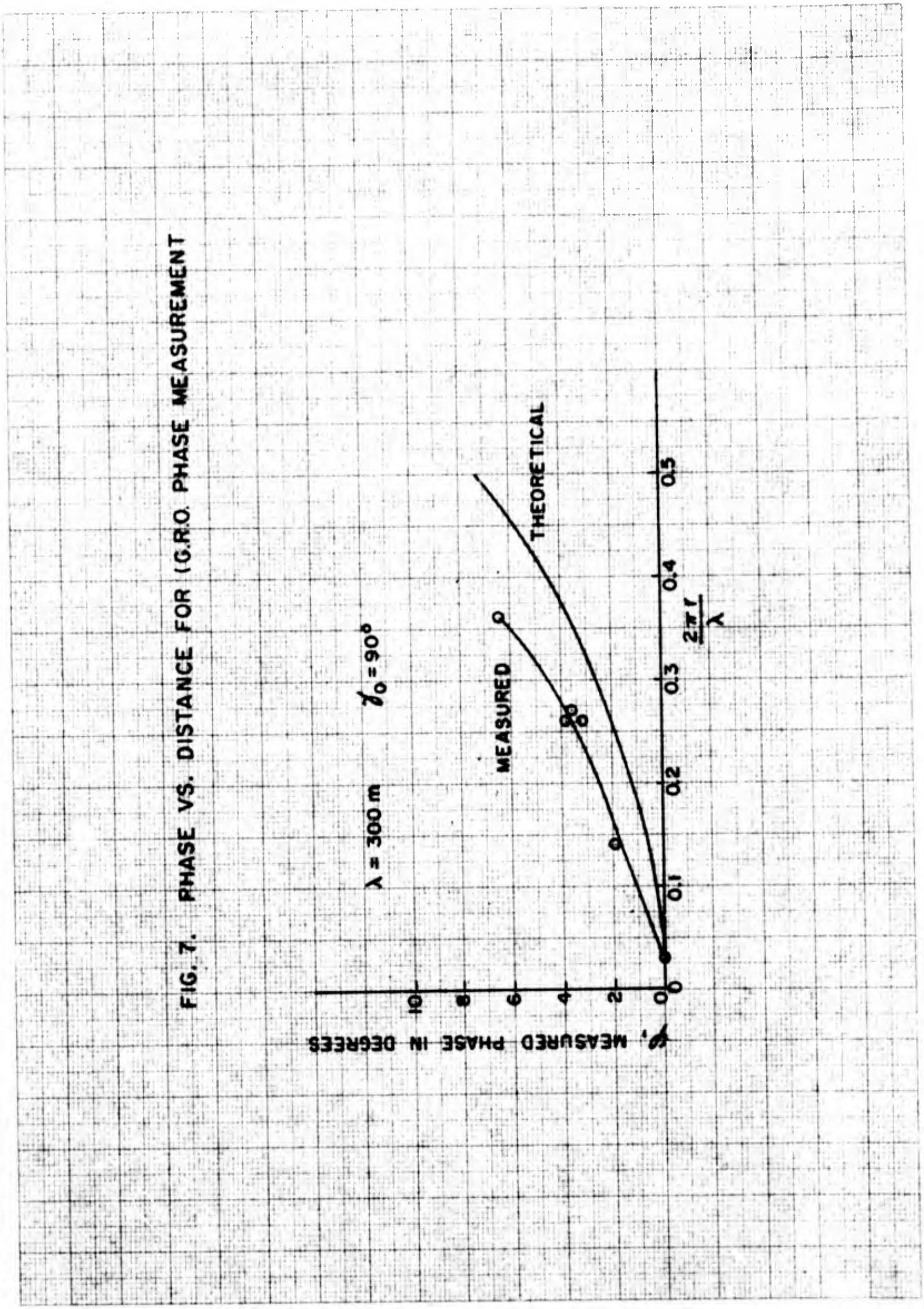
FIG. 7. PHASE VS. DISTANCE FOR (G.R.O. PHASE MEASUREMENT
λ = 300 m
γ0 = 90°
MEASURED
THEORETICAL
90°
0
φ, MEASURED PHASE IN DEGREES
2πr/λ
0
2
4
6
8
10
0.1
0.2
0.3
0.4
0.5

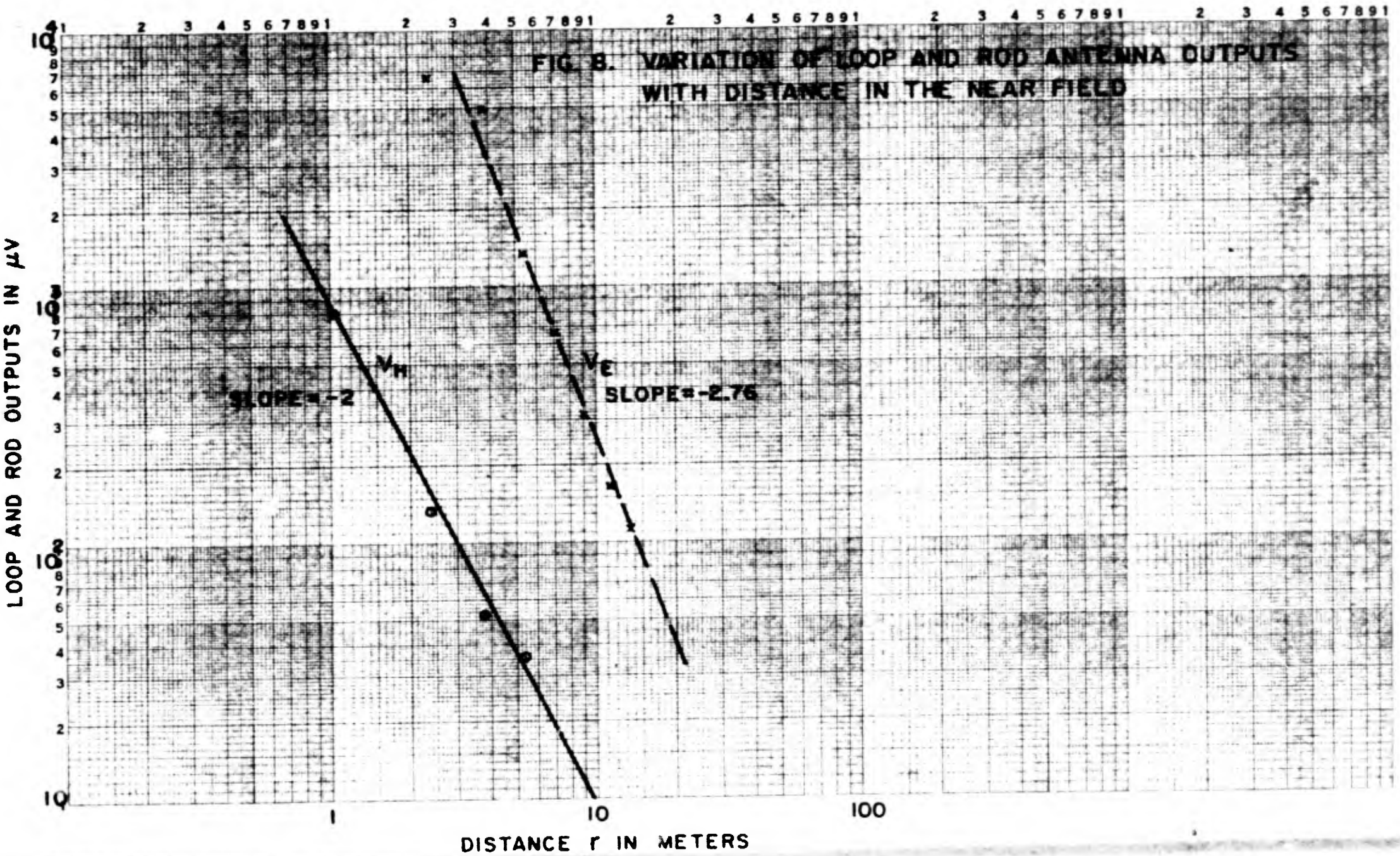

FIG. 8. VARIATION OF LOOP AND ROD ANTENNA OUTPUTS WITH DISTANCE IN THE NEAR FIELD

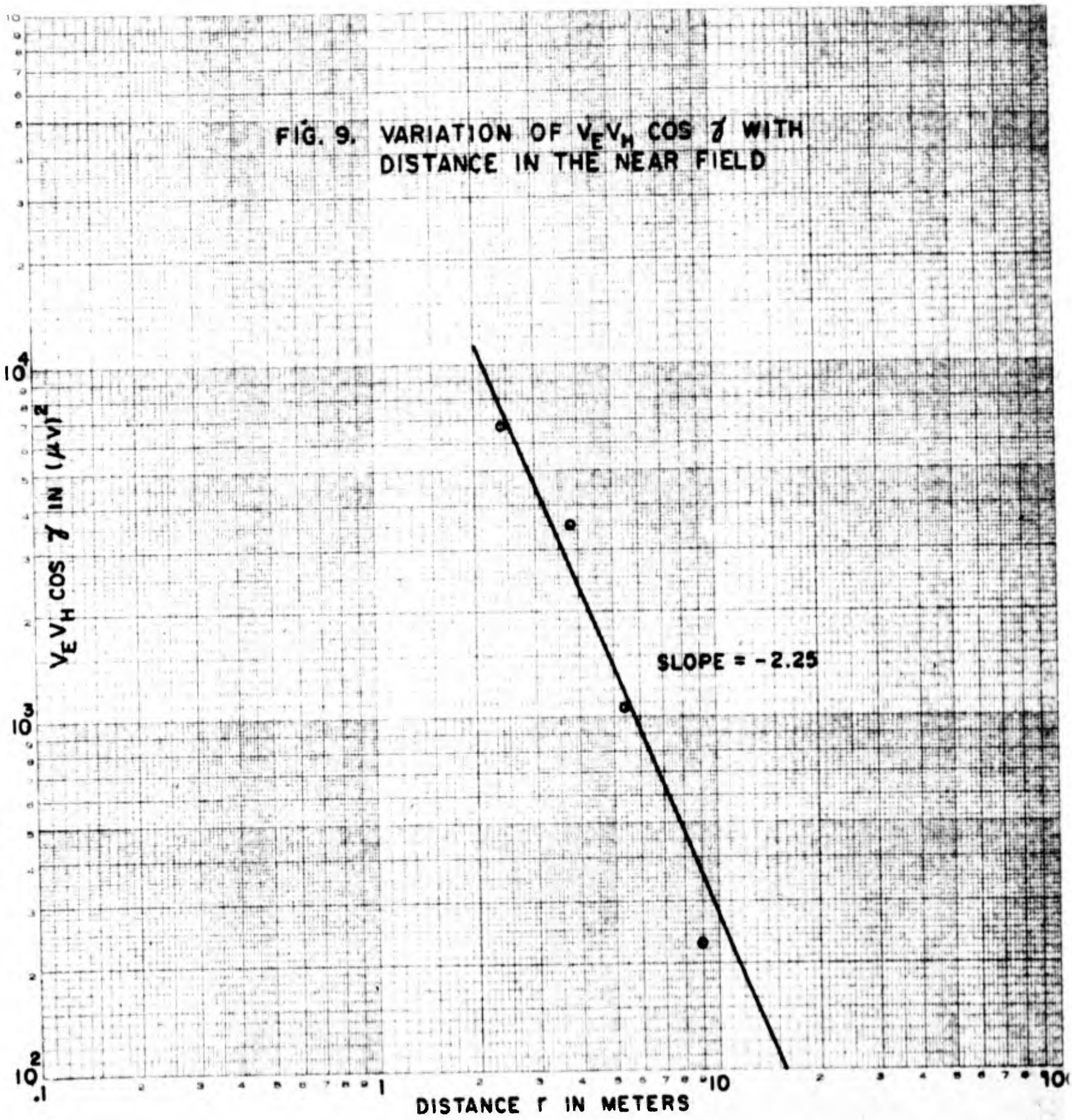

FIG. 9. VARIATION OF $V_E V_H \cos \gamma$ WITH DISTANCE IN THE NEAR FIELD

our disposal, zero phase difference can be obtained at the outputs of the two PRM-1's, and can be readily seen on the oscilloscope.

In this manner, the outputs are "tuned" to zero phase difference. The actual phase difference between E_θ and H_φ is then 90° minus the measured phase change. γ_o in this case is 90°. Using the results of Fig. 7 and Fig. 8 which give the amplitude variation of V_E and V_H with distance, one can compute the variation of the quantity $V_E V_H \cos \gamma$, which is proportional to the magnitude of the Poynting vector with distance. The results of this computation are shown in Fig. 9, which indicates an almost inverse square law dependence in agreement with theory.

4.0 PHASE MEASUREMENT WITH A TRANSISTORIZED PHASEMETER

Since the results of the measurements given in the previous section justify a refinement in the phase measurement technique, it was decided to build and test a portable phasemeter according to a circuit furnished by Mr. Brooks of the U. S. Naval Civil Engineering Laboratory, Port Hueneme, Calif., which is reproduced in Fig. 10. Since this circuit has been described elsewhere,[3] we shall only include the results of measurement performed with the meter and its calibration.

The design specifications of the phasemeter are as follows:

Frequency range	20 kc-2Mc
Input Impedance	2 kΩ
Input voltages	1-2 volts
Accuracy, nominal	5%

Calibration

Due to the lack of an appropriate phase shifter or delay line, the phasemeter was calibrated using a scheme very similar to that used in the test and calibration of the multiplier. The IF output voltages e_{S1} and

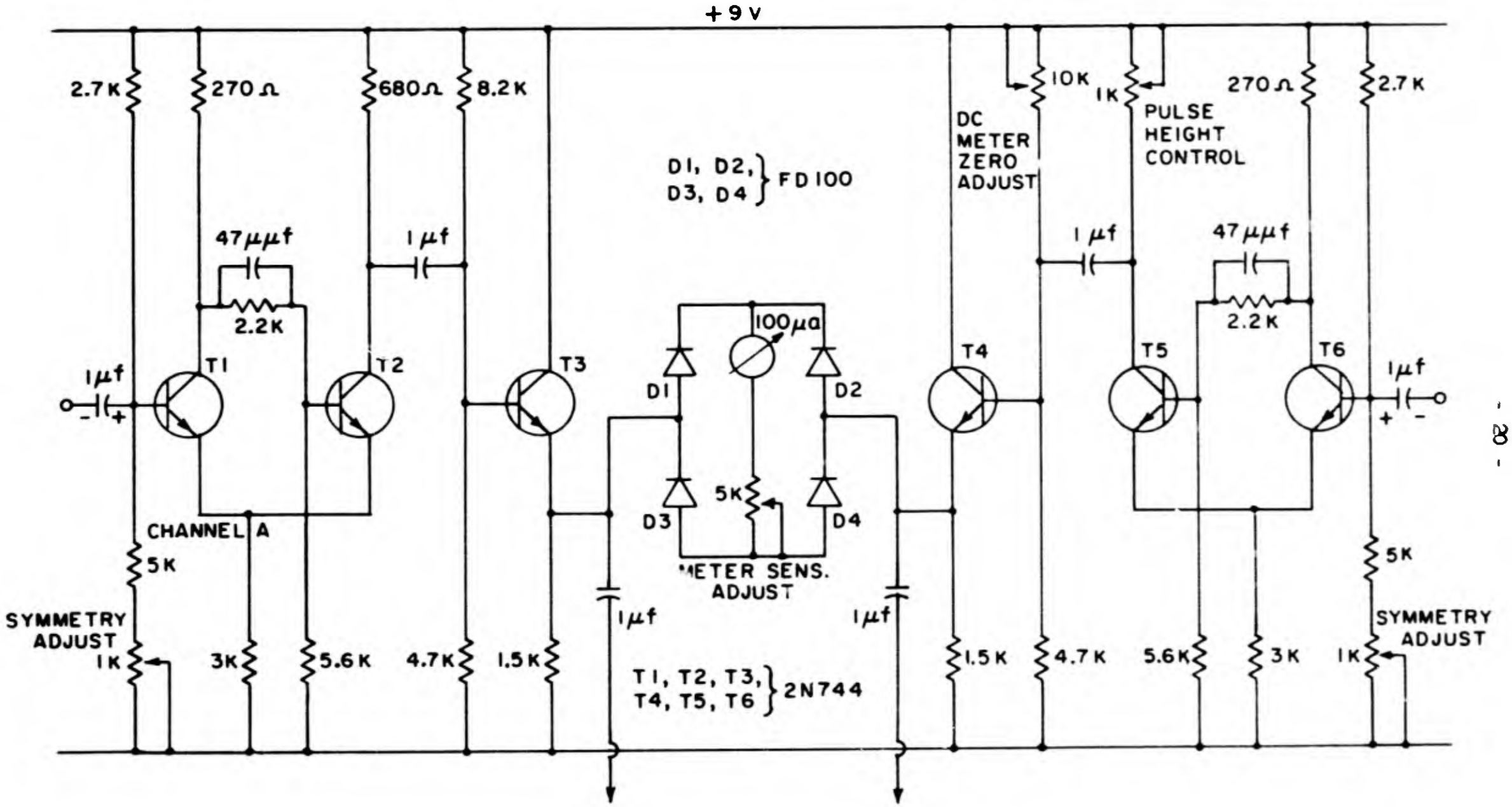

FIG. 10. CIRCUIT DIAGRAM OF PHASE METER

e_{S2} (see Fig. 3) were fed to the two inputs of the phasemeter. The phase between these voltages was varied from 0° to 180° in steps of 10° each, monitored on the scope, by retuning the slave receiver. The magnitudes of e_{S1} and e_{S2} were maintained constant at 2 volts by making use of the gain control knobs on the receivers (the position of the step attenuator was kept constant all through calibration since it was found that changing its position on either receiver changes slightly the relative phase between e_{S1} and e_{S2}). The experimental setup for calibration is that shown in Fig. 3, with the exception of the multiplier which was replaced by the phasemeter. The phase between the two input signals to the phasemeter was measured by the dual beam CRO. The results of the calibration are shown in Fig. 11. The calibration curve does not drop to zero at zero phase, apparently due to the noise of the receivers. The calibration curve is not linear; it shows that the phasemeter has maximum sensitivity for angles between 20° - 100°. This fact was later utilized in the actual phase measurement in the field. Accuracy of the phase reading on the meter was within one degree.

Measurement

The experimental setup used to perform the measurement in the field is essentially that given in Fig. 5, with the exception that the multiplier is now replaced by the transistorized phasemeter. It was initially intended to use the step attenuators and the continuous gain control knobs on the PRM-1 receivers to maintain the magnitudes of the IF signals fed to the phasemeter constant (at a value between 1 to 2 volts according to design recommendations) as the distance between transmitter and the sensor was changed, and to record V_E and V_H in addition to the phasemeter reading. However, since shifting the position of the step attenuators on either receiver

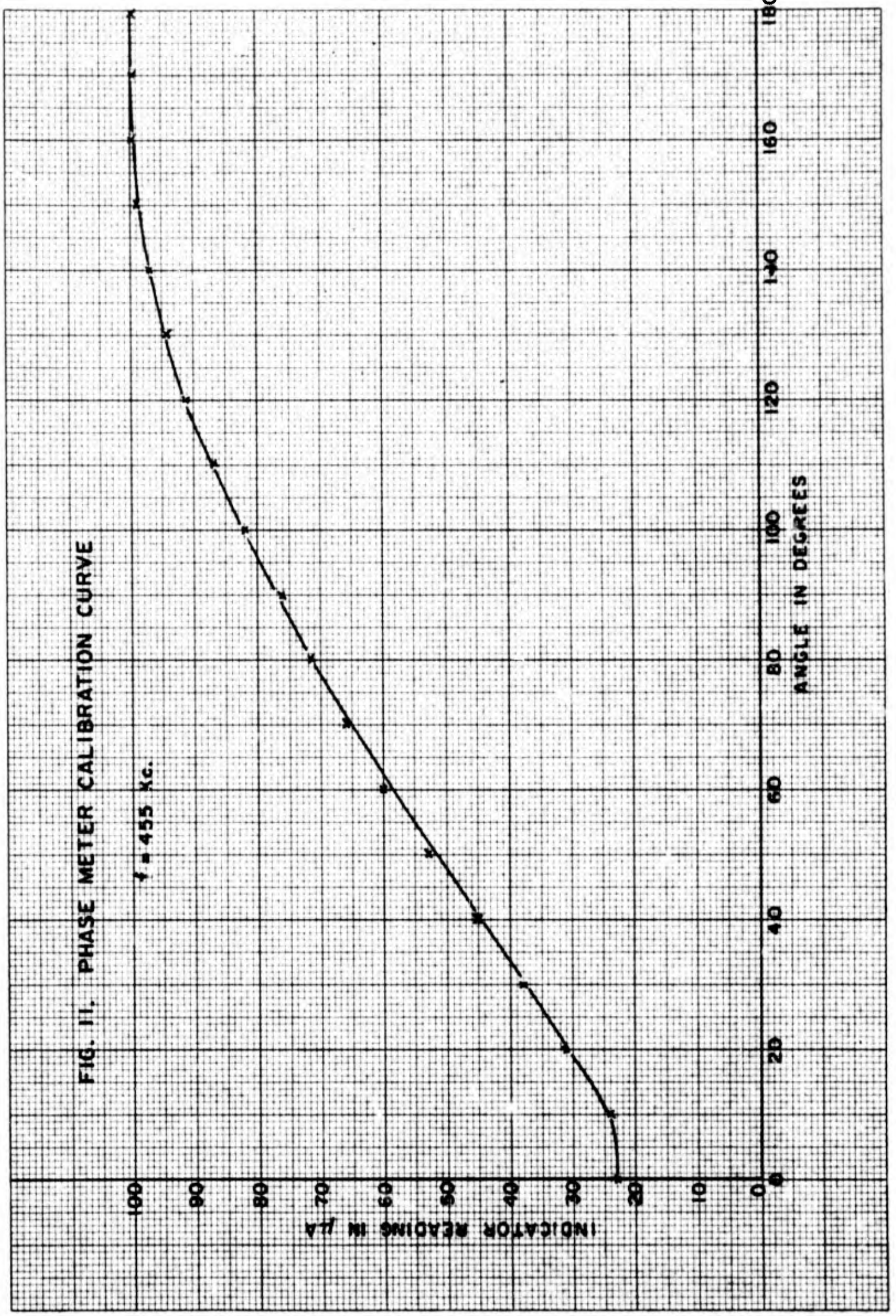

FIG. III. PHASE METER CALIBRATION CURVE

is known to introduce a slight phase shift between the IF signals, this scheme of measurement was abandoned. The difficulty was overcome by making use of the fact that the operation of the phasemeter was to all practical purposes virtually independent of the input signal levels for signals above 2 volts rms. Thus, the actual measurement was performed with the position of the step attenuators fixed (on zero attenuation). This provided input signals to the phasemeter in excess of 2 volts for distances within 30 meters from the transmitter.

Since the time phase between the IF output voltages of the PRM-1 receivers is dependent on the position of the step attenuators, it has been found advantageous and more accurate to measure the amplitudes and phase difference separately. The amplitude measurements are as described in the phase measurement section with the scope (see Fig. 5). The results of this measurement are given in Table IV and are shown in Fig. 12.

With regard to phase difference measurement, a certain phase is deliberately introduced so that the phasemeter may be operated in its linear region. Measurements are made at various distances and the phasemeter readings in μA's are converted into phase angle degrees by means of the calibration curve. In mapping one of the measurement points on the theoretical curves, the constant is easily found. For example, at 5 meters we know that the phase difference between E and H is about 89.6° (see Fig. 4.4.3, Ref. 2). In changing the measured value to match the theoretical value at this point and the other values by the same amount, the desired curve is obtained. This is shown in Fig. 13, also columns 5, 6 and 7 in Table IV.

TABLE IV

Measurement of $V_E V_H \cos \gamma$

(Phase measured with transistorized phasemeter)

Run #	Distance in meters	V_E in μv	V_H in μv	Phase Meter Reading in μv	Phase in degrees from calibr. chart	γ^o	$V_E V_H \cos \gamma$
1	5	5.2×10^3	1.03×10^3	80	97	89.6	3.75×10^4
	10	9.0×10^2	3.3×10^2	80.5	97.5	-	-
	15	2×10^2	1.2×10^2	78.8	95	87.6	1.0×10^3
	20	7.2×10^1	9×10^1	76.6	91.5	84.1	6.67×10^2
	25	4.0×10^1	4.5×10^1	75	90	82.6	2.12×10^2
	30	2.2×10^1	2.8×10^1			-	-
2	5	5.2×10^3	1.03×10^3	81.5	100	89.6	3.72×10^4
	10	9.0×10^2	3.3×10^2	81	98.5	88.1	9.87×10^3
	15	2×10^2	1.2×10^2	79.8	96.5	86.1	1.63×10^3
	20	7.2×10^1	9×10^1	76.5	91.5	81.1	1.0×10^3
	25	4.0×10^1	4.5×10^1	73.8	86	75.6	4.1×10^2
	30	2.2×10^1	2.8×10^1	68.5	74.5	-	-
3	5	5.2×10^3	1.03×10^3	65	69.5	89.6	3.72×10^4
	10	9.0×10^2	3.3×10^2	64.5	68.5	88.6	7.25×10^3
	15	2×10^2	1.2×10^2	63.5	66.5	86.6	1.43×10^3
	20	7.2×10^1	9×10^1	61.5	63	83.0	7.9×10^2
	25	4.0×10^1	4.5×10^1	58.5	58	78.1	3.4×10^2
	30	2.2×10^1	2.8×10^1	54	50	-	-

FIG. 12. VARIATION OF LOOP AND ROD ANTENNA OUTPUTS WITH DISTANCE

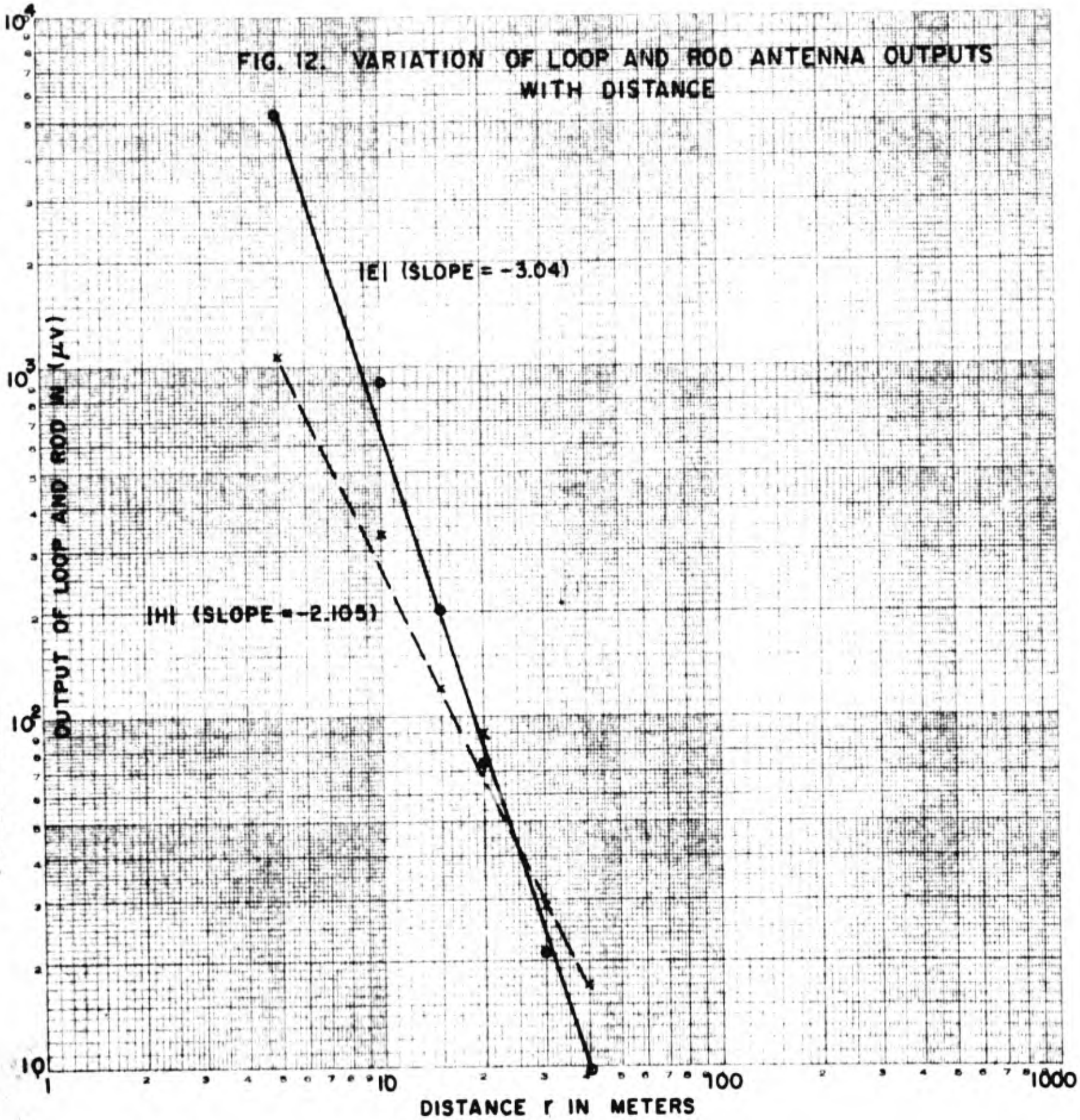

FIG. 13. PHASE VS. DISTANCE FOR THREE TYPICAL RUNS
(TRANSISTORIZED PHASE METER)

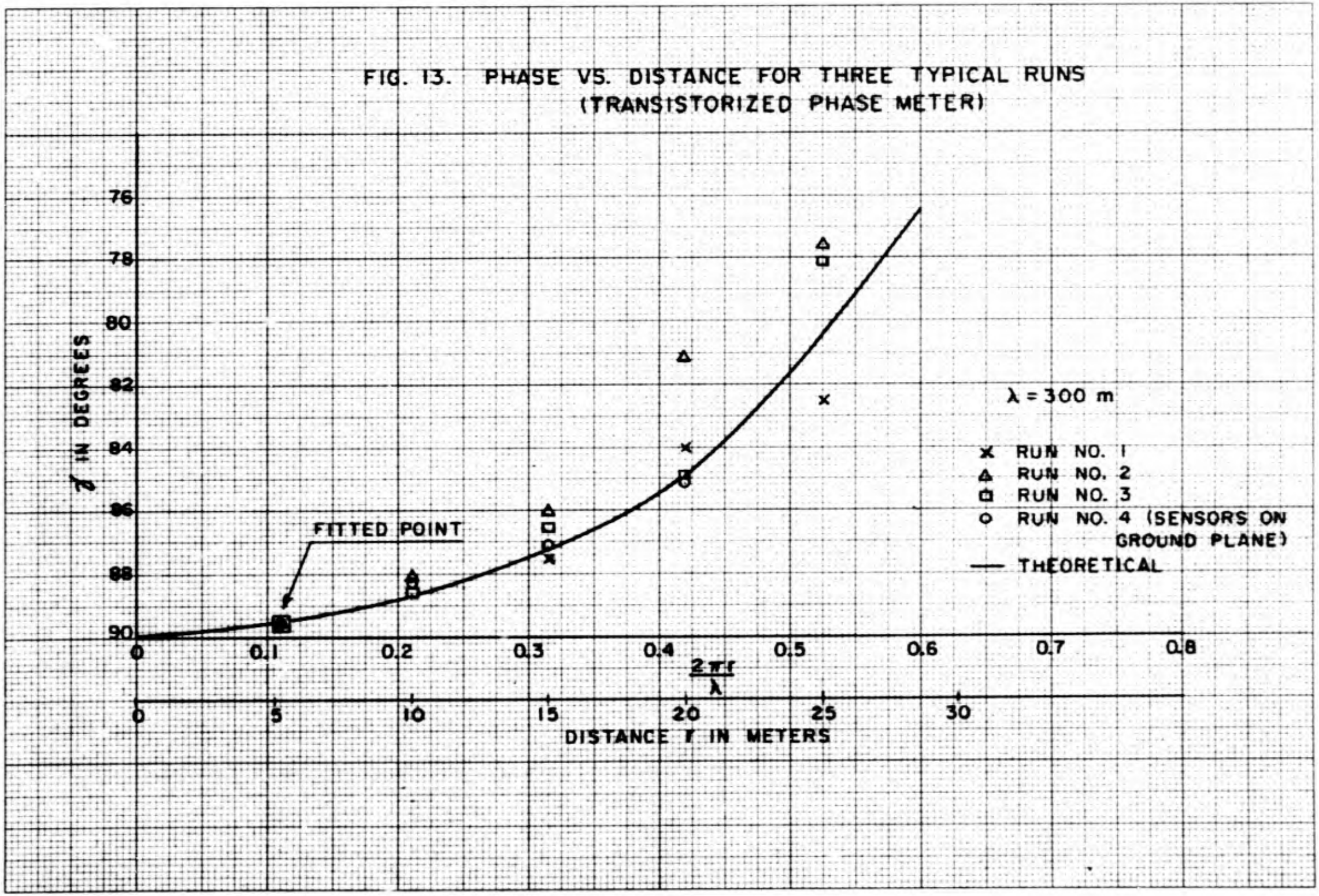

Having obtained the magnitudes of V_E and V_H, and their phase difference at various distances, the quantity $V_E V_H \cos \gamma$ is computed. The variation of this quantity with distance is shown in Fig. 14 for two typical runs. The slopes are - 2.25 and - 2.35, which is in close agreement with the expected theoretical inverse square law.

5.0 EFFECT OF GROUND PLANE

The measurements described above were performed when the rod and loop antennas were mounted directly on the PRM-1 receivers. The measurement was repeated when the sensors were installed on a small ground plane, approximately 1 meter × 1/2 meter, and their outputs conveyed through cables underneath the plane to the receivers. The results of this measurement are given in Table V. The variation of the quantity $V_E V_H \cos \gamma$ with distance for this case is shown in Fig. 15, which indicates a slope of - 2.38.

One can conclude that a ground plane under the Poynting sensor can only serve to eliminate the effects of the cables on the measurement. It has no evident major effect on the final results of the measurement.

6.0 CONCLUSIONS

The experiments and results presented in this report indicate that Poynting vector measurement at 1 Mc is feasible. It can be achieved either by measuring the loop and rod antenna output voltage (V_H and V_E) and the time phase between them separately or directly through the use of a multiplier, from whose output a quantity proportional to the magnitude of the Poynting vector can be derived. The results of either method of measurement are in general agreement with theoretical prediction. With the exception of slightly lowering the loop and rod output voltages, no effect was evident on the measurement when a ground plane was installed under the Poynting sensor.

The multiplier, although far from being ideal, can lead through further development to an instrument which can provide the magnitude of the Poynting vector with greater ease. This can be greatly enhanced by either eliminating the dependence of a_o and a_2 on the magnitudes of the input signals or by incorporating the multiplier with a number of additional networks (step and continuous attenuators and transistorized amplifiers) which will insure equal inputs to the multiplier without affecting the phase difference between these inputs--a thing that could not be achieved with the PRM-1 receivers.

7.0 FUTURE PROGRAM

During the next three months the following investigations will be carried out:

1) Consideration will be given to the improvement of the multiplier in order to obtain a more satisfactory direct reading device.

2) The availability of item 1 will make it possible to measure certain broadband signals; for example, a rapidly repeated impulse generator. It is pointed out that all tests and theory associated with this work to date have been confined to sine wave sources.

3) Measurements will be carried out on certain "different" noise sources. Included, for example, will be a straight wire parallel to the earth whose length is large compared with the spacing between the wire and the Poynting measuring device. Also, devices having various ratios of E to H will be tested, including a set of large capacitor plates and a large resonant loop.

8.0 REFERENCES

1. Cowles, W. W., K. S. Foo and R. M. Showers, "Study of Methods of Implementing Poynting Vector Measurement," Moore School of Electrical Engineering, University of Pennsylvania, Report #64-23, January 1 to March 31, 1964.

2. Bartfeld, R. A., et al., "Feasibility Study of Poynting Vector Measurements," Moore School of Electrical Engineering, University of Pennsylvania, Interim Report No. 4, April 1 to June 30, 1963.

3. Brooks, J. L., "Low Frequency Current-Probe System for Measuring Conducted Radio Frequency Interference," Technical Report R-304, June 25, 1964, U. S. Naval Civil Engineering Laboratory, Port Hueneme, Calif.

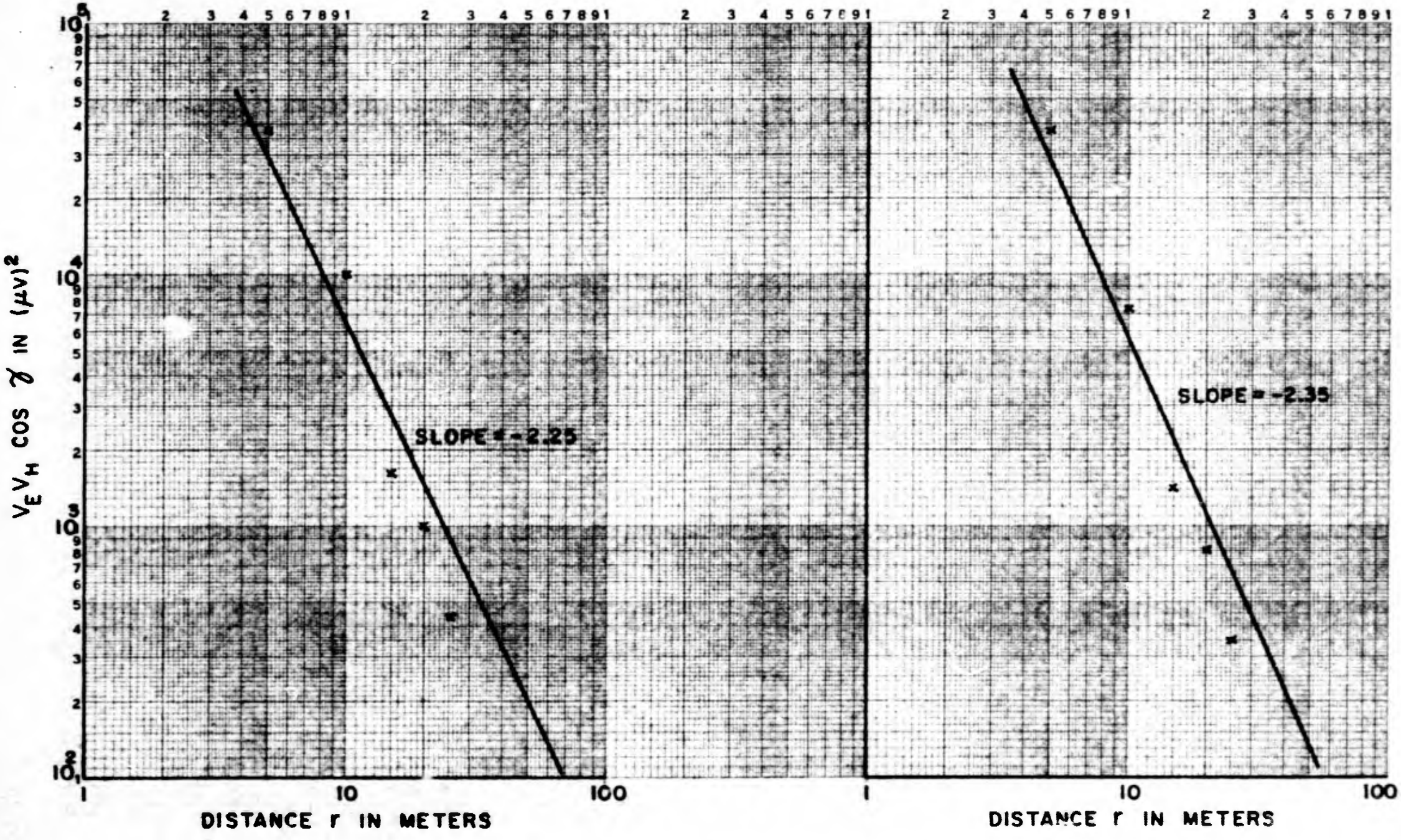

FIG. 14. VARIATION OF $V_E V_H \cos\gamma$ WITH DISTANCE FOR TWO TYPICAL RUNS – 2 AND 3

TABLE V

Measurement of $V_E V_H \cos \gamma$ with Poynting Sensor on Ground Plane
(Phase measured with transistorized phasemeter)

Run No.	Distance in meters	V_E in μv	V_H in μv	Phase in μA	Phase in Degrees	γ	$V_E V_H \cos \gamma$
1	5	100 × 10	100 × 10	72	81.5	89.6^o	6.98×10^3
	10	22.5 × 10	26 × 10	71.5	80	88.1^o	1.87×10^3
	15	7.3 × 10	12.5 × 10	71	79	87.1^o	4.67×10^2
	20	3 × 10	7.5 × 10	69.5	77	85.1^o	1.92×10^2

FIG. 15. VARIATION OF $V_E V_H \cos \psi$ WITH DISTANCE WHEN POYNTING SENSOR IS MOUNTED OVER GROUND PLANE

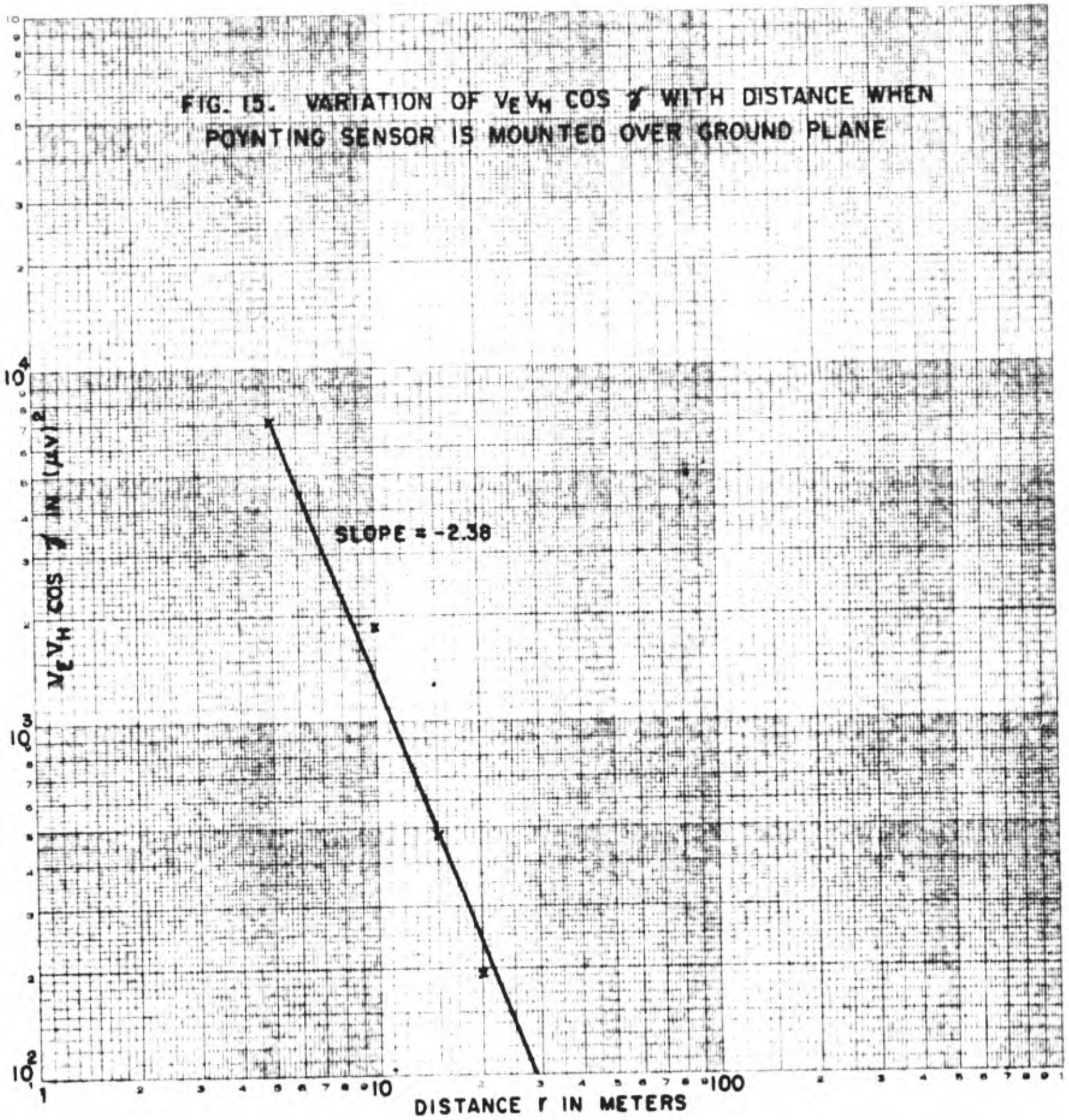

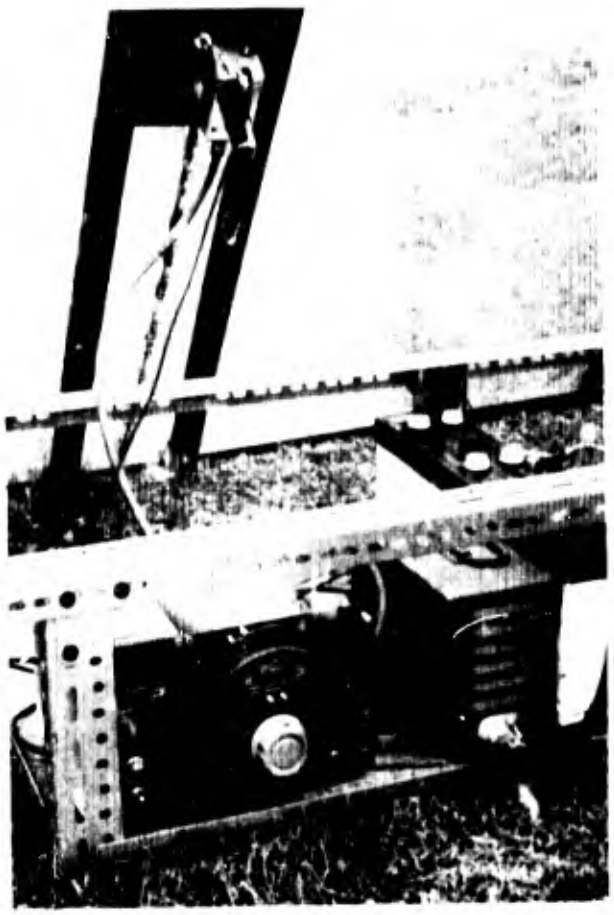

(a)

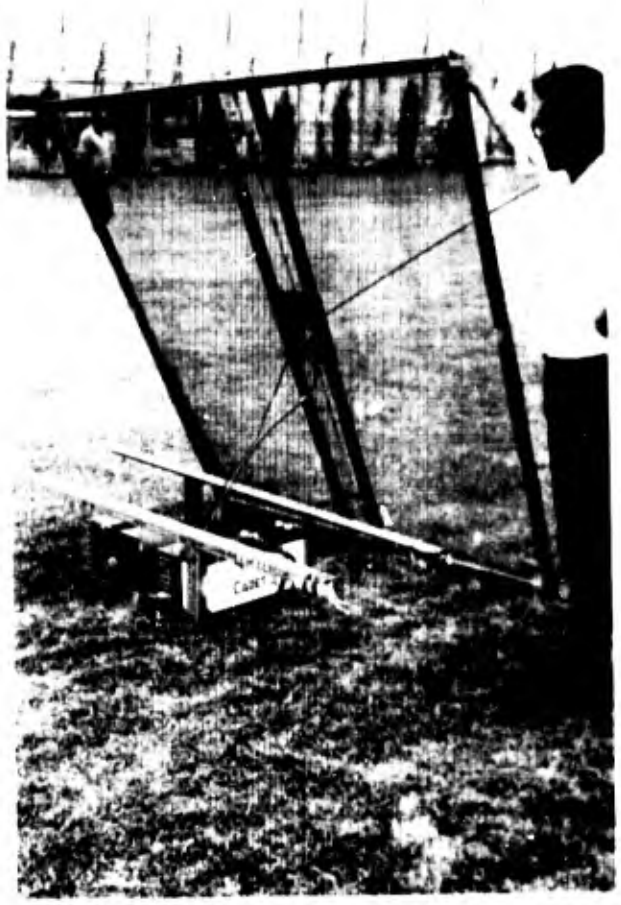

(b)

(c)

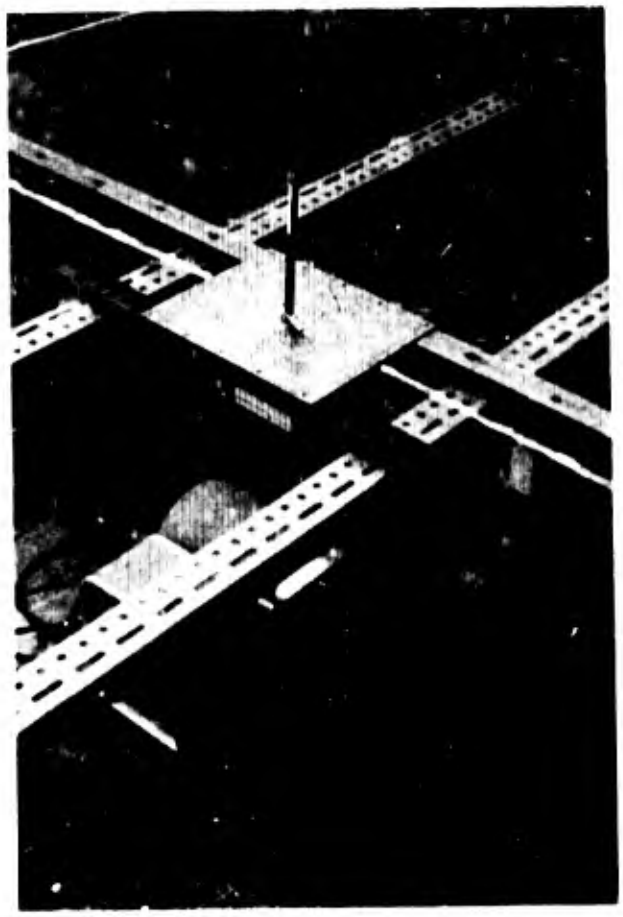

(d)

Figure 16 - Transmitter. (a) Transmitter and Power Pack, (b) Transmitter Antenna and Ground Plane, (c) 1 Mc Power Amplifier, (d) Transmitter under Ground Plane.

(c)

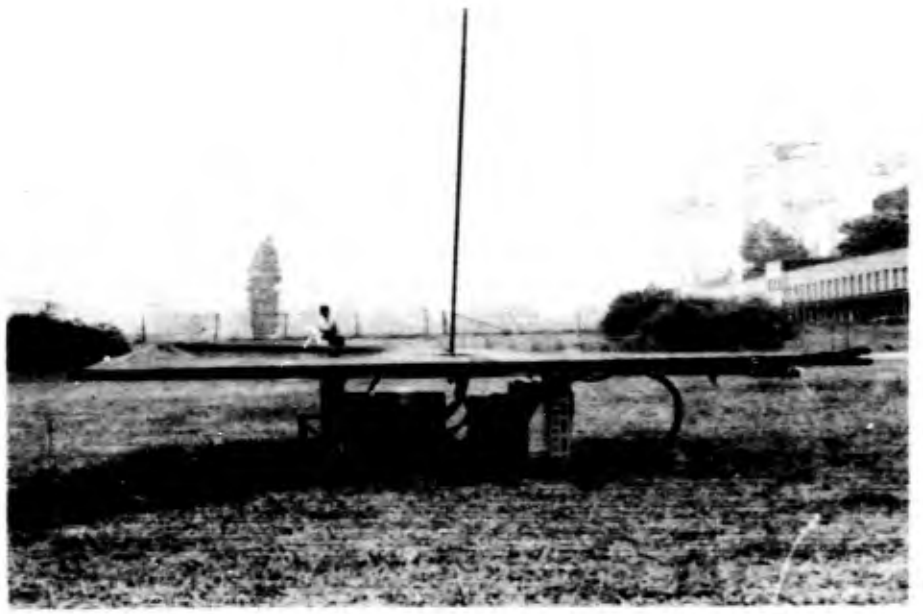

(a)

(b)

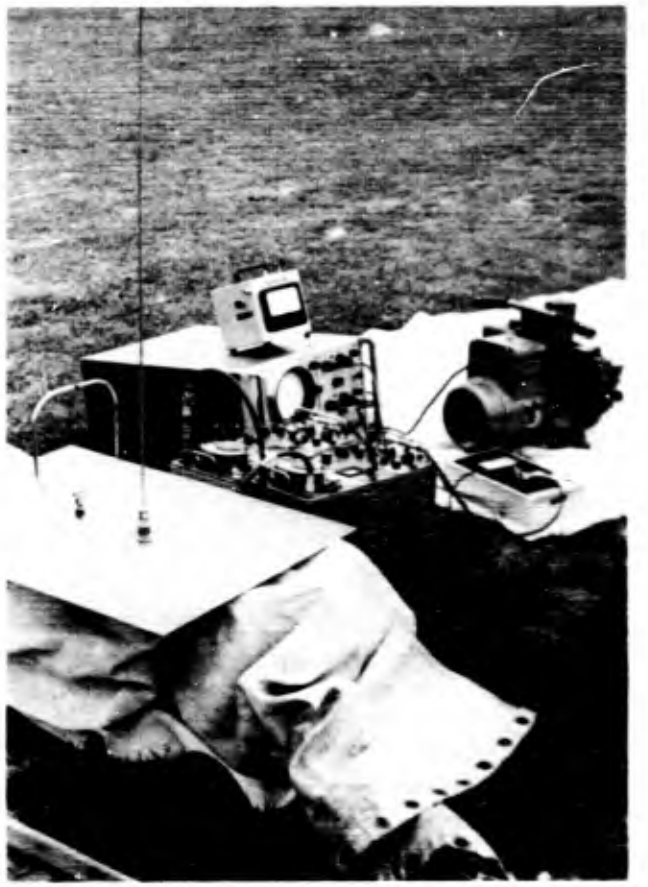

Figure 17. Poynting Vector Measurement System.
(a) Transmitter Assembly.
(b) Poynting Sensor System Showing Sensor on Ground Plane, PRM-1 Receivers, Phasemeter, Multiplier Oscilloscope with ac Power Pack.
(c) Transmitter and Poynting Sensor Systems.

(a)

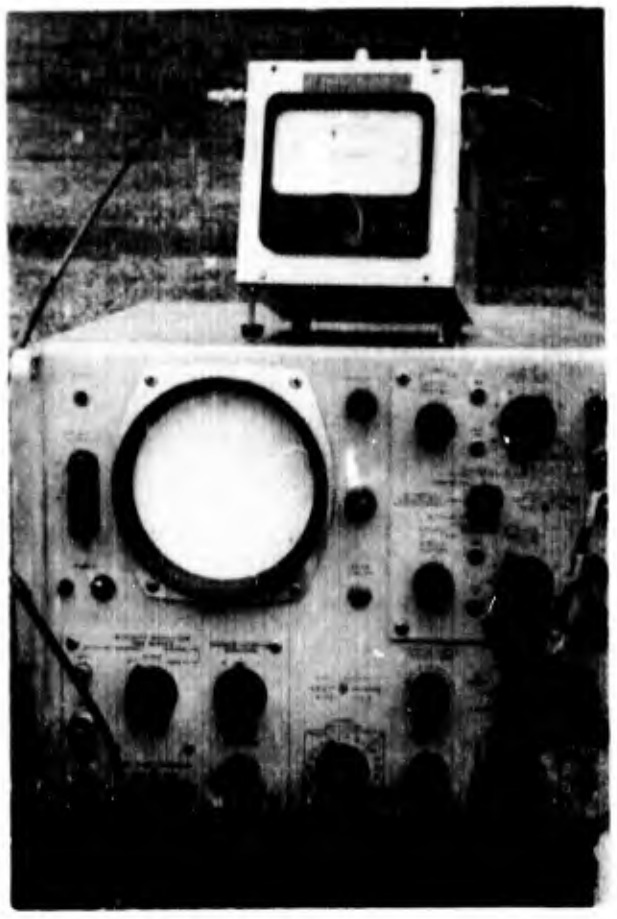

(b)

Figure 18. (a) Phasemeter, (b) Phasemeter showing reading proportional to phase difference between voltages displayed on the oscilloscope.

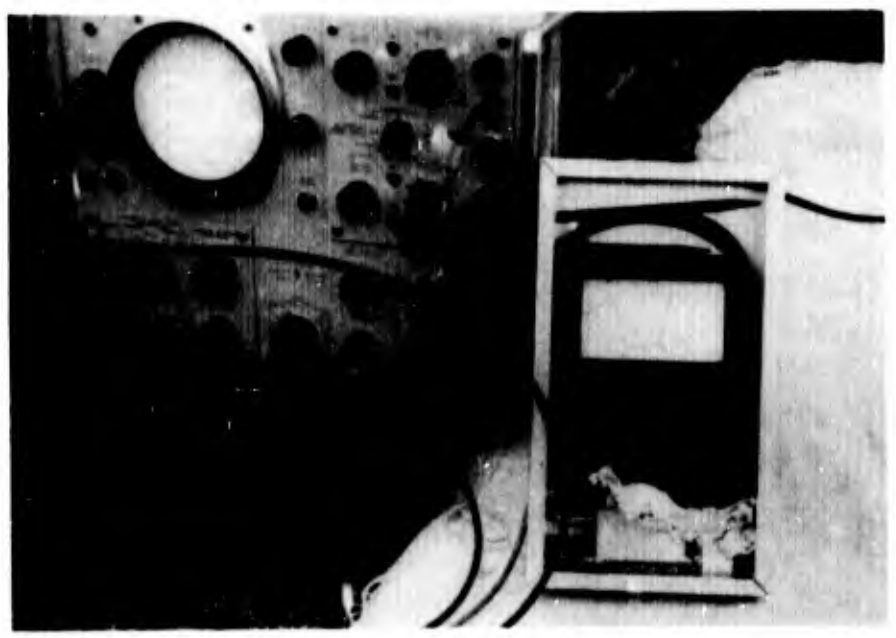

Figure 19. Multiplier

BLANK PAGE